Computed Tomographic Measures of Pulmonary Vascular Morphology in Smokers and Their Clinical Implications

Raúl San José Estépar[1,2,3], Gregory L. Kinney[4], Jennifer L. Black-Shinn[4], Russell P. Bowler[5], Gordon L. Kindlmann[6], James C. Ross[3,7], Ron Kikinis[1,2], MeiLan K. Han[8], Carolyn E. Come[7], Alejandro A. Diaz[7], Michael H. Cho[7,9], Craig P. Hersh[7,9], Joyce D. Schroeder[10], John J. Reilly[11], David A. Lynch[10], James D. Crapo[12], J. Michael Wells[13], Mark T. Dransfield[13], John E. Hokanson[4], and George R. Washko[7]; for the COPDGene Study

[1]Department of Radiology, [2]Surgical Planning Laboratory, [3]Laboratory of Mathematics in Imaging, [7]Division of Pulmonary and Critical Care, and [9]Channing Division of Network Medicine, Department of Medicine, Brigham and Women's Hospital, Boston, Massachusetts; [4]Department of Epidemiology, Colorado School of Public Health, University of Colorado, Denver, Colorado; [5]Division of Pulmonary and Critical Care Medicine, and [10]Department of Radiology, National Jewish Health, Denver, Colorado; [6]Department of Computer Science, University of Chicago, Chicago, Illinois; [8]Division of Pulmonary and Critical Care, University of Michigan, Ann Arbor, Michigan; [11]Department of Medicine, University of Pittsburgh/UPMC, Pittsburgh, Pennsylvania; [12]Department of Medicine, National Jewish Medical and Research Center, Denver, Colorado; and [13]Division of Pulmonary and Critical Care, University of Alabama at Birmingham, Birmingham, Alabama

Rationale: **Angiographic investigation suggests that pulmonary vascular remodeling in smokers is characterized by distal pruning of the blood vessels.**

Objectives: **Using volumetric computed tomography scans of the chest we sought to quantitatively evaluate this process and assess its clinical associations.**

Methods: **Pulmonary vessels were automatically identified, segmented, and measured. Total blood vessel volume (TBV) and the aggregate vessel volume for vessels less than 5 mm^2 (BV5) were calculated for all lobes. The lobe-specific BV5 measures were normalized to the TBV of that lobe and the nonvascular tissue volume (BV5/$T^{issue}V$) to calculate lobe-specific BV5/TBV and BV5/$T^{issue}V$ ratios. Densitometric measures of emphysema were obtained using a Hounsfield unit threshold of −950 (%LAA-950). Measures of chronic obstructive pulmonary disease severity included single breath measures of diffusing capacity of carbon monoxide, oxygen saturation, the 6-minute-walk distance, St George's Respiratory Questionnaire total score (SGRQ), and the body mass index, airflow obstruction, dyspnea, and exercise capacity (BODE) index.**

Measurements and Main Results: **The %LAA-950 was inversely related to all calculated vascular ratios. In multivariate models including age, sex, and %LAA-950, lobe-specific measurements of BV5/TBV were directly related to resting oxygen saturation and inversely associated with both the SGRQ and BODE scores. In similar multivariate adjustment lobe-specific BV5/$T^{issue}V$ ratios were inversely related to resting oxygen saturation, diffusing capacity of carbon monoxide, 6-minute-walk distance, and directly related to the SGRQ and BODE.**

Conclusions: **Smoking-related chronic obstructive pulmonary disease is characterized by distal pruning of the small blood vessels (<5 mm^2) and loss of tissue in excess of the vasculature. The magnitude of these changes predicts the clinical severity of disease.**

Keywords: pulmonary vasculature morphology; CT scan; smoking; COPD

AT A GLANCE COMMENTARY

Scientific Knowledge on the Subject

Angiographic investigation suggests that pulmonary vascular remodeling in smokers is characterized by distal pruning of the blood vessels. Computed tomographic imaging may allow quantitative assessments of this process.

What This Study Adds to the Field

Clinically relevant pulmonary vascular remodeling in smokers manifests as distal pruning of the intraparenchymal blood vessels and a disproportionate loss of nonvascular tissue in regions of emphysema. Further exploration of these processes may lead to new therapies in smokers.

It is estimated that 30–70% of subjects with chronic obstructive pulmonary disease (COPD) have clinically significant pulmonary vascular disease (1–4). There are, however, few therapies available for this disease despite it being associated with increased use of healthcare resources and being an independent predictor of mortality (5–10). Reasons for this include the inability to perform detailed studies of pulmonary vascular disease in large cohorts of smokers and limited understanding of who is at greatest risk of suffering from such disease.

As ascertained by early roentologic investigation, angiography, and necropsy, there are several types of macroscopic pathologic pulmonary vascular changes possible in smokers. These aberrant morphologies reflect several processes including inflammatory remodeling with progressive luminal occlusion, vessel elongation in regions of hyperinflation, and outright loss of vasculature in regions of severe emphysematous destruction (11–18). The structural manifestations of such processes have a deleterious impact on blood flow.

Tools that are currently available to assess the pulmonary vasculature, such as histologic examination and right heart

(*Received in original form January 25, 2013; accepted in final form April 12, 2013*)

Supported by NHLBI grants K25 HL104085-03 and 1R01HL116931-01 (R.S.J.E.), K23HL093351-04 (M.K.H.), and K23HL089353-05 and 1P50HL107192 (G.R.W.). The COPDGene Study is supported by NHLBI grants 2R01HL089897-06A1 (PI: J.D.C.), 2R01HL089856-06A1 (PI: Edwin Silverman), and R01HL116473 (G.R.W. and R.S.J.E.).

Author Contributions: Conception and design, R.S.J.E., G.L.K., J.L.B.-S., J.E.H., and G.R.W. CT analysis, R.S.J.E., J.J.R., G.L.K., and R.K. Analysis and interpretation, R.S.J.E., G.L.K., J.L.B.-S., J.E.H., and G.R.W. Drafting the manuscript for important intellectual content, R.S.J.E., R.P.B., R.K., M.K.H., C.E.C., A.A.D., M.H.C., C.P.H., J.D.S., J.J.R., D.A.L., J.D.C., J.M.W., M.T.D., J.E.H., and G.R.W.

Correspondence and requests for reprints should be addressed to George R. Waskho, M.D., Division of Pulmonary and Critical Care Medicine, Department of Medicine, Brigham and Women's Hospital, 75 Francis St, Boston, MA 02115. E-mail: gwashko@partners.org

This article has an online supplement, which is accessible from this issue's table of contents at www.atsjournals.org

Am J Respir Crit Care Med Vol 188, Iss. 2, pp 231–239, Jul 15, 2013
Copyright © 2013 by the American Thoracic Society
Originally Published in Press as DOI: 10.1164/rccm.201301-0162OC on May 8, 2013
Internet address: www.atsjournals.org

catheterization (RHC), are too invasive to perform on large numbers of subjects. Further, RHC, echocardiography, and measures of single breath diffusing capacity of carbon monoxide (D_{LCO}) suffer from significant limitations. Just as FEV_1 cannot discern the relative admixture of emphysema and airway disease in COPD (both thought to be highly relevant predictors of disease manifestations, such as rate of decline in lung function or acute exacerbations of disease [19–22]), RHC, echocardiography, and D_{LCO} lack the ability discern the types of pathologic vascular remodeling present and their regional distribution.

Computed tomographic (CT) imaging of the chest may be able to quantitatively assess macroscopic pulmonary vascular morphology in smokers and how it may be associated with outcomes in COPD. Using data from a subset of subjects enrolled in the COPDGene Study we sought to obtain CT-based assessments of pulmonary vasculature morphology among subjects with varying degrees of expiratory airflow obstruction and then examine their clinical associations. Based on our prior investigation (23, 24) we hypothesized that those smokers with the greatest distal pruning of the vasculature measured by a decrease in their distal vascular blood vessel volume would have the greatest clinical impairment.

METHODS

Study Population

The COPDGene Study has been described in detail previously. The study enrolled a total of 10,362 subjects; an interim analysis was planned after enrollment of the first 2,500 subjects (25). For our current investigation we focused on three groups of subjects within the COPDGene Study. The first group included 359 smokers, from the first 2,500 subjects, who were enrolled in a single center, National Jewish Health, and had complete CT data. This subset was selected to minimize the impact of variable scanner brands, generations, and image reconstruction parameters on measures of vascular morphology. The second group included 82 never-smokers with normal lung function (26) and no history of lung disease for whom we had measures of vascular morphology. These subjects were recruited from several centers in the COPDGene Study network as described previously (26). The third group was comprised of 16 subjects who, against study protocol, enrolled and were CT scanned twice in the study. All of these subjects except two went to the same study center for their second enrollment. The repeat scans were done within 6 months of the first scan and we selected those subjects whose total lung capacity on follow-up was within 200 ml of the first scan.

CT Scan Examination

Standardized volumetric CT scans of the chest were performed at full inspiration using the COPDGene Study imaging protocol with 120 kVp, 200 mAs, and 0.5 rotation time. The smoking group was scanned at a single center using two scanning platforms: GE LightSpeed 16 (GE, Milwaukee, WI) and Siemens Definition (Siemens, Munich, Germany). The never-smoker control subjects were scanned using GE LightSpeed 16, GE Discovery HD750, Siemens Definition, Siemens Definition AS+, or Siemens Definition Flash. Images were reconstructed using a standard algorithm at 0.625-mm slice thickness and 0.625-mm intervals for the GE scanner. Siemens CT images were reconstructed using a B31f algorithm at 0.75-mm slice thickness and 0.5-mm intervals.

Clinical and Physiologic Assessments

Oxygen saturation was measured using pulse oximetry with the subject seated at rest breathing ambient gas. Spirometric measures of lung function were performed using the Easy-One spirometer (ndd Medical Technologies, Inc., Andover, MA) before and after the administration of a short-acting inhaled bronchodilator per American Thoracic Society recommendations and expressed as a percent of predicted values for age, height, race, and sex (27, 28). Exercise capacity was assessed by the maximal distance a subject could walk in 6 minutes (6-MWD). Data from the St. George's Respiratory Questionnaire (SGRQ) provided measures of disease-related health impairment, with a higher total score suggesting greater disease impact and lower quality of life (29).

Using the spirometric measures of lung function, Modified Medical Research Council dyspnea score (30), body mass index, and 6-MWD, the body mass index, airflow obstruction, dyspnea, and exercise capacity (BODE) multidimensional index to predict mortality in COPD was calculated (31). Post-bronchodilator measures of D_{LCO} ($n = 139$) were obtained in a subset of this cohort.

CT Scan Analysis

Volumetric CT scans of the chest were performed at maximal inflation. Densitometric measures of emphysema using a Hounsfield unit threshold of −950 (%LAA-950) and lung lobe segmentation were performed using Airway Inspector (www.AirwayInspector.org) (32, 33). The pulmonary vasculature was automatically segmented from the parenchyma using in-house software (additional detail on the method for extracting these measurements is provided in the online supplement) (34, 35). Assessments of pulmonary vascular morphology included total blood vessel volume (TBV) in the combined intraparenchymal pulmonary arteries and veins and the aggregate blood vessel volume in vessels less than 5 mm^2 in cross-section (BV5) for the whole lung and lung lobe. This latter 5 mm^2 cutoff was based on prior investigation (23, 24, 36). Given the inherent anatomic variability in blood vessel volume (i.e., taller people have a greater blood vessel volume) the BV5 measures were normalized by expressing them as ratios of the TBV (i.e., $BV5_{RUL}/TBV_{RUL}$) of that lobe of interest.

The lobe-specific measures of BV5 were also normalized by the nonvascular tissue volume ($T^{issue}V$) (i.e., $BV5_{RUL}/T^{issue}V_{RUL}$) of that same lobe of interest. This latter ratio was created to examine the symmetry or asymmetry of tissue and blood vessel loss in emphysematous parenchyma. To do this the total volume and the volume of emphysematous tissue for each lobe were ascertained. Subtraction of the volume of emphysema from the total lobe volume provided a measure of tissue volume, which included the vasculature; subtraction of the TBV from that value resulted in a measure of the nonvascular tissue volume for the lobe. Vascular analysis was performed independently in all lung lobes and the right and left lung. The right upper (RUL) and right lower lobe (RLL) were selected to assess clinical correlates of the lobe-specific vascular analysis. Data and clinical associations for the remaining lobes are presented in the online supplement and referenced where appropriate. The COPDGene Study was approved by the Institutional Review Boards of all participating centers, and written informed consent was obtained from each subject before his or her enrollment. Subjects with symmetrically reduced FEV_1 and FVC and a preserved FEV_1/FVC ratio (Global Initiative for Chronic Obstructive Lung Disease [GOLD] U) were excluded from this analysis (37).

Statistical Analysis

Data are presented as means ± SD or medians and interquartile range where appropriate. Pulmonary vascular morphology was analyzed as a continuous covariate and was expressed as a measure of whole lung or lobar blood volumes (i.e., TBV_{global}, $BV5_{global}$, TBV_{RUL}, $BV5_{RUL}$, and so forth) and lobar vessel volumes normalized for either the lobar total blood volume or the lobar total nonvascular tissue volume. Lobe-specific ratios for the BV5 adjusted by the TBV in that same lobe are designated as the $BV5_{RUL}/TBV_{RUL}$ and $BV5_{RLL}/TBV_{RLL}$ for the RUL and RLL, respectively. Similarly, lobe-specific ratios of the BV5 to total nonvascular tissue volume in that same lobe are designated as the $BV5_{RUL}/T^{issue}V_{RUL}$ and $BV5_{RLL}/T^{issue}V_{RLL}$, respectively.

A signed-rank test of the difference in BV5 quantities was used to compare reproducibility in the 16 subjects with repeat CT scans. Nonparametric methods were used to assess differences in blood vessel volume among groups, whereas linear regression was used to evaluate trends across GOLD stages. Univariate (Pearson) and multivariate linear regression were used to examine the relationship between CT measures of pulmonary vascular morphology and %LAA-950, resting oxygen saturation, D_{LCO}, the 6-MWD, and SGRQ total score. The relationship between CT measures of pulmonary vascular morphology and BODE index was assessed with ordinal logistic regression. The odds reported

are for a one SD reduction in the $BV5_{RUL}/TBV_{RUL}$, $BV5_{RLL}/TBV_{RLL}$, $BV5_{RUL}/T^{issue}V_{RUL}$, and $BV5_{RLL}/T^{issue}V_{RLL}$ being associated with a one point increase in BODE score. The proportional odds assumption was assessed for each model using chi-square. Multivariate models were adjusted for age, sex, race, height (centimeter), weight (kilogram), %LAA-950, and FEV_1 percentage predicted (FEV_1pp) unless otherwise specified. Statistical analysis was performed using SAS 9.3 (Carey, NC). *P* values less than 0.05 were considered statistically significant.

RESULTS

In the cohort of 16 subjects with repeat CT scans, there was no intrasubject difference in BV5 measures ($P = 0.2$). The clinical characteristics of the never-smoking normals and smoker cohort from National Jewish Health are provided in Table 1. Volumetric models of the intraparenchymal pulmonary vasculature were created for each subject (examples shown in Figure 1) and lobe-specific plots of the distribution of vessel volume as a function of vessel cross-sectional area were generated (Figure 2).

Right upper and right lower blood vessel volumes for the never smokers and smokers are presented in Table 2 (remaining lung lobe data are provided in Table E1 of the online supplement). There was no difference in the median blood vessel volume measures between the never-smokers and smoking control subjects or between current and former smoking control subjects ($P > 0.05$; data not shown). In the smokers there was no significant trend observed with the TBV_{Global}, TBV_{RUL}, or TBV_{RLL}, but the measures of BV5 and nonvascular tissue volume were decreased in subjects with higher GOLD stages of disease.

Ratios of BV5 to TBV and $T^{issue}V$ are presented in Table 3 (*see* Table E2) for never-smoking control smokers. For the RUL and LUL there were significant differences in the BV5 to $T^{issue}V$ ratio between the never-smokers and smoking control subjects. No similar difference was noted with the BV5/TBV ratios. In the smokers, the ratios of BV5 to TBV for all the lobes decreased with increasing GOLD stage, whereas there was no similar relationship between GOLD stage and the BV5 to $T^{issue}V$ ratios. The BV5 to TBV ratio was directly related to the FEV_1pp ($r = 0.36$, $P < 0.0001$ and $r = 0.39$, $P < 0.0001$ for the RUL and RLL, respectively). Similar associations between FEV_1pp and the BV5 to $T^{issue}V$ ratios were not seen.

The TBV_{global} and the $BV5_{global}$ were directly related to the total lung volume calculated from the CT scan ($r = 0.48$, $P < 0.0001$ and $r = 0.36$, $P < 0.0001$, respectively). Similar associations were observed for lobe-specific blood vessel volumes and the volume of the RUL and RLL (TBV_{RUL}, $r = 0.53$, $P < 0.0001$; $BV5_{RUL}$, $r = 0.42$, $P < 0.0001$) and (TBV_{RLL}, $r = 0.41$, $P < 0.0001$; $BV5_{RLL}$, $r = 0.40$, $P < 0.0001$). The $BV5_{global}$ was directly related to the TBV_{global} for the total lung ($r = 0.91$; $P < 0.0001$) and the $BV5_{RUL}$ and $BV5_{RLL}$ were directly related to the TBV_{RUL} and TBV_{RLL} ($r = 0.95$, $P < 0.0001$ and $r = 0.91$, $P < 0.0001$, respectively). Furthermore, all vascular measures (TBV_{global}, $BV5_{global}$, $BV5_{RUL}/TBV_{RUL}$, $BV5_{RLL}/TBV_{RLL}$, $BV5_{RUL}/T^{issue}V_{RUL}$, and $BV5_{RLL}/T^{issue}V_{RLL}$) were inversely related to %LAA-950 (Table 4; *see* Table E8). We then explored the associations between clinical measures of disease severity and CT-assessed intraparenchymal vasculature.

There was no significant association between the D_{LCO} and either the $BV5_{RUL}/TBV_{RUL}$ or $BV5_{RLL}/TBV_{RLL}$; however, vessel measures normalized for the nonvascular tissue volume were significantly and inversely related to the D_{LCO} (Table 4) and remained so in multivariate regression after adjustment for sex, %LAA-950, height (centimeter), and age (years) (Table 5; *see* Table E3). The $BV5_{RUL}/TBV_{RUL}$ and the $BV5_{RLL}/TBV_{RLL}$ were directly related to resting oxygen saturation, whereas the $BV5_{RUL}/T^{issue}V_{RUL}$ and $BV5_{RLL}/T^{issue}V_{RLL}$ were inversely related to resting oxygen saturation (Table 4). These observations held in additional multivariate analysis (Table 5; *see* Table E4).

After examining the relationships between pulmonary blood vessel volume and both the D_{LCO} and resting oxygen saturation we sought to examine the associations of blood vessel volume and its distribution with the 6-MWD, SGRQ total score, and BODE score. Based on the trends observed in the vascular measures across GOLD stages, we hypothesized that those with the lowest ratio of distal blood volume to total blood volume and those with the greatest ratio of distal blood volume to nonvascular tissue volume would have the most clinical impairment.

The $BV5_{RUL}/TBV_{RUL}$ and $BV5_{RLL}/TBV_{RLL}$ were directly related to the 6-MWD, whereas the $BV5_{RUL}/T^{issue}V_{RUL}$ and $BV5_{RLL}/T^{issue}V_{RLL}$ were inversely related to the 6-MWD (Table 4). In models adjusted for FEV_1pp, %LAA-950, sex, height (centimeter), weight (kilogram), and age, lobe-specific BV5/$T^{issue}V$ but not BV5/TBV remained significant (Table 5; *see* Table E5). The $BV5_{RUL}/TBV_{RUL}$ and $BV5_{RLL}/TBV_{RLL}$ were associated with a decreased SGRQ total score, whereas $BV5_{RUL}/T^{issue}V_{RUL}$ but not $BV5_{RLL}/T^{issue}V_{RLL}$ ($P = 0.068$) was associated with an increase in the SGRQ total score in the univariate analysis (Table 4). The associations to SGRQ total score with lobe-specific BV5/$T^{issue}V$ ratios held in the multivariate model after adjustment for FEV_1pp, %LAA-950, sex, and age except for the RLL, and lobe-specific BV5/TBV ratios were not associated with SGRQ total score except for the RUL (Table 5; *see* Table E6).

Finally, we examined the relationships between our vascular measures and BODE index. Reductions in $BV5_{RUL}/TBV_{RUL}$ and $BV5_{RLL}/TBV_{RLL}$ were associated with a higher BODE score (Table 4), whereas neither $BV5_{RUL}/T^{issue}V_{RUL}$ nor $BV5_{RLL}/T^{issue}V_{RLL}$ was associated with BODE score. After adjustment for %LAA-950, sex, and age the associations with $BV5_{RUL}/TBV_{RUL}$ and $BV5_{RLL}/TBV_{RLL}$ remained (odds ratio, 1.8; 95% confidence interval, 1.2–2.7; $P = 0.003$; and odds ratio, 2.3; 95% confidence interval, 1.5–3.5; $P < 0.0001$, respectively) (Table 5; *see* Table E7).

TABLE 1. DATA DISTRIBUTION FOR THE SUBJECT GROUPS USED IN THIS STUDY

	Never-Smoking Control Subjects (*n = 85*)	Smokers (*n = 359*)
Female sex	—	185
Age, yr	62.4 (56.3–69.1)	63.7 (54.6–70.1)
FEV_1 % predicted	103.7 (93–113)	59 (38–89)
Height, cm	163.2 (159.5–171.6)	168.7 (163.0–176.1)
Weight, kg	80.2 (63.8–88.5)	78.6 (64.3–90.0)
BMI	27.5 (24.1–31.4)	26.65 (23.08–30.70)
%LAA-950	0.8 (0.4–2.3)	6.33 (1.75–22.76)
Oxygen saturation	—	93 (90–95)
6-MWD, ft	—	1310 (1,025–1,650)
SGRQ total score	—	32.16 (15.94–47.26)
BODE (n = 352)	—	2 (0–4)
D_{LCO} (n = 135)	—	13.11 (8.58–16.64)

Definition of abbreviations: %LAA-950 = percentage of low-attenuation areas less than −950 Hounsfield units; 6-MWD = 6-minute-walk distance; BMI = body mass index; BODE = body mass index, airflow obstruction, dyspnea, and exercise capacity index; D_{LCO} = diffusing capacity of carbon monoxide; SGRQ = St. George's Respiratory Questionnaire.

DISCUSSION

We have previously reported a measure of pulmonary vascular morphology termed the cross-sectional area (23, 24). This method consisted of a two-dimensional analysis of axial CT images based on the assumption that all "round" structures represented vessels captured in long axis to the CT scanning plane. The total cross-sectional area of those structures was

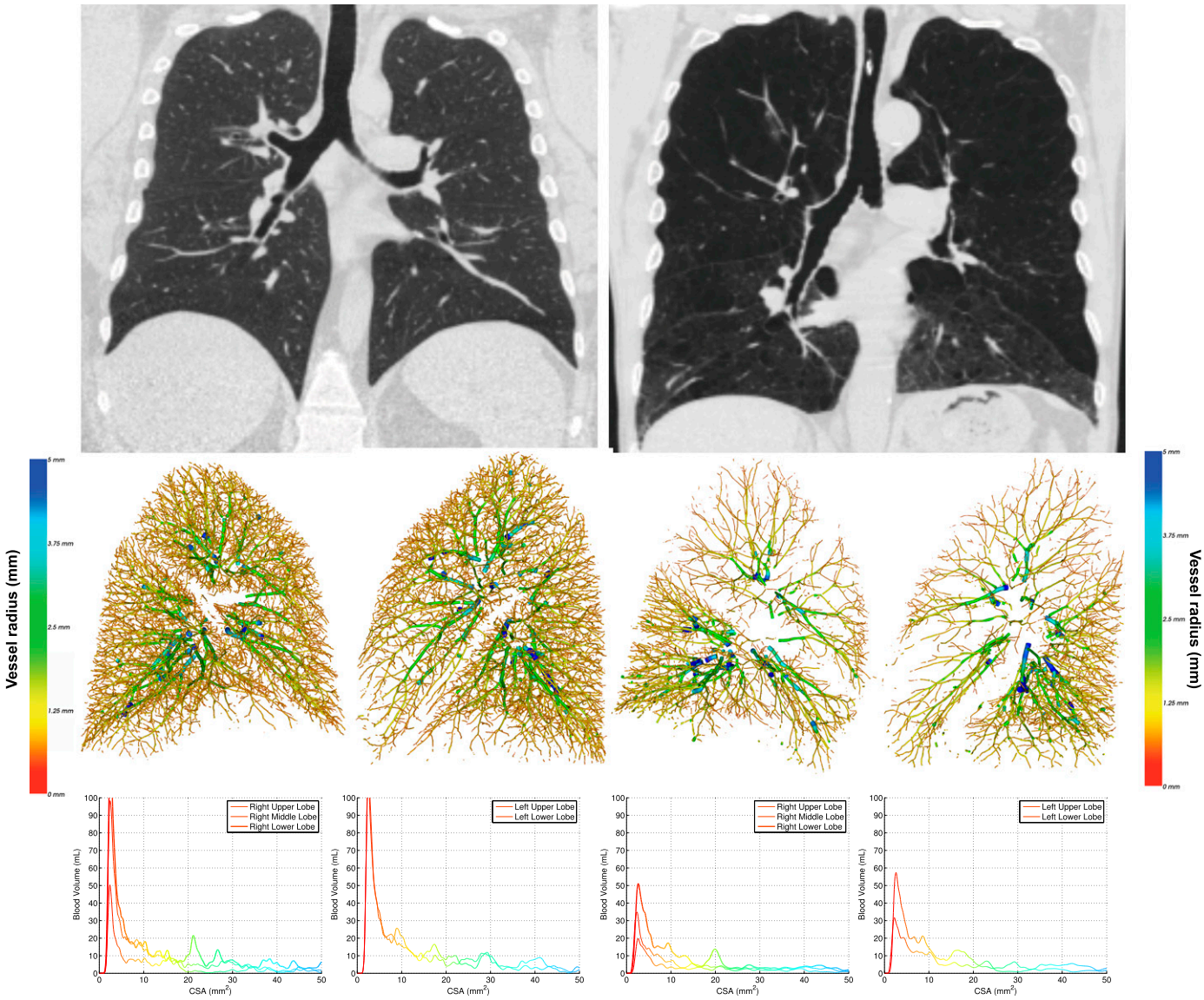

Figure 1. (*Top*) Coronal images of a never-smoker (*left*) and smoker with Global Initiative for Chronic Obstructive Lung Disease 4 chronic obstructive pulmonary disease (*right*). (*Middle*) Volumetric reconstructions of the pulmonary vasculature that are color-coded based on vessel radii. (*Bottom*) Distribution of blood vessel volume as a function of the cross-sectional area (CSA) of the vessels. Plots are color-coded based on vessel size as shown in the volumetric models of the vasculature. The larger peaks in the plots in the CSA range of 0–10 mm^2 suggest that most intraparenchymal blood vessel volume is within the vessels whose CSA is 0–10 mm^2. All plots are the same scale. Note the effect of emphysema on the size of the blood vessel volume peak in the 0–10 mm^2 CSA range.

then normalized by the area of lung in the axial scanning plane. Although this measure continues to perform well on standard high-resolution CT there are certain limitations, such as the potential inclusion of nonvascular structures in the analysis and the assumption that data from three axial slices are representative of the entire lung. Additionally, one may question if the clinical relevance of the cross-sectional area measures is driven by the aggregate area of the vessels; the cross-sectional area of the lung (which would be increased in states of hyperinflation); or a combination of the two. To begin to explore these questions we developed a technique to automatically segment and create a three-dimensional model of the intraparenchymal pulmonary vasculature. Using these models we calculated absolute measures of blood vessel volume and lobe-based ratios of distal blood vessel volume to the total intraparenchymal blood vessel volume. We also created lobe-based ratios of distal blood vessel volume to the total nonvascular tissue volume, all with the intent of exploring the association of these measures to the resting oxygen saturation, D_{LCO}, 6-MWD, SGRQ total score, and BODE score. We believed that the breadth of these clinical measures and their potential association with blood vessel morphology as assessed by CT scanning could provide more insight into pulmonary vascular disease in smokers.

Our first measures of the pulmonary vasculature included the TBV and BV5. We found that those subjects with more CT evidence of emphysema had a lower TBV and BV5. These observations are not surprising because angiographic studies of smokers reported a loss of vasculature in regions severely affected by emphysema and narrowing of the remaining segmental and subsegmental vessels (11, 12). The diminution of intraparenchymal blood vessel volume and presumably the intraparenchymal blood volume may proceed centripetally toward the hilum and be

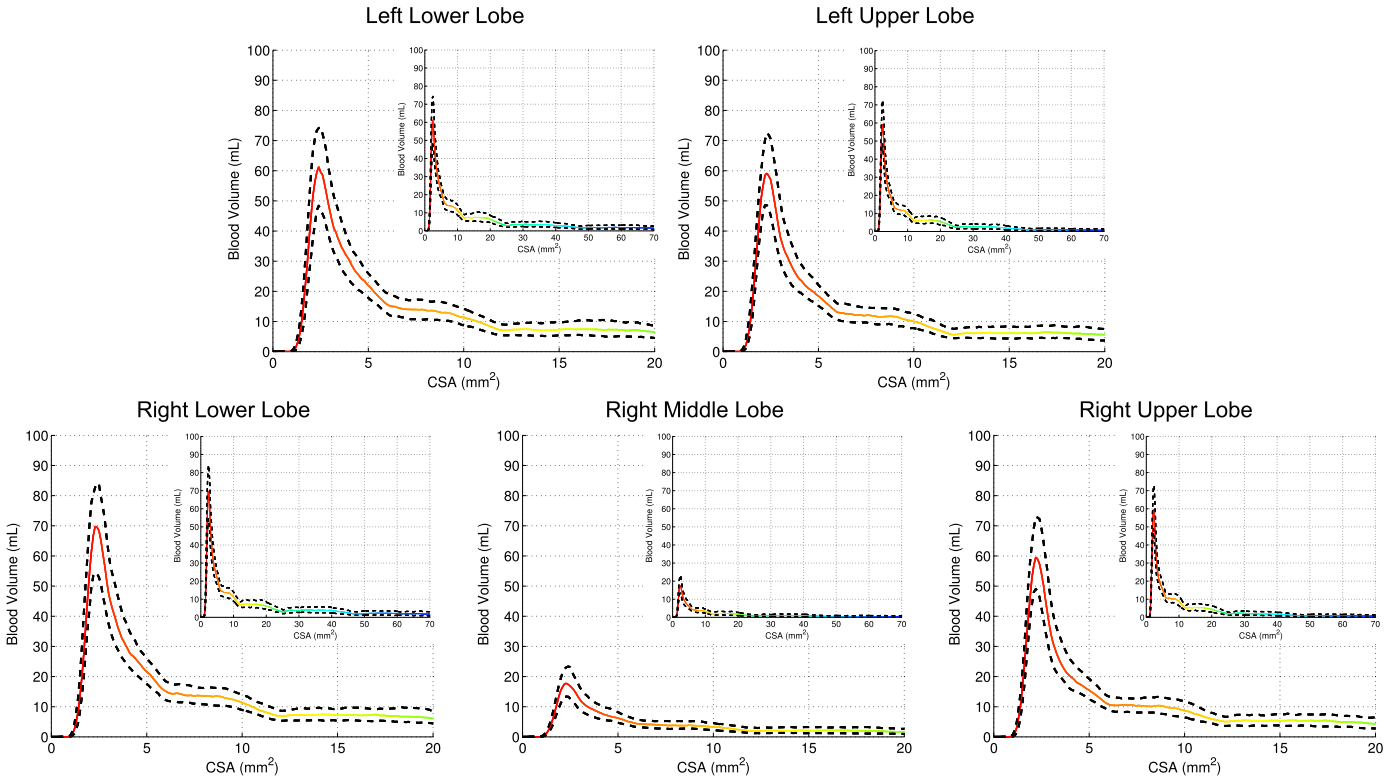

Figure 2. Summary profiles for the blood vessel volume as a function of blood vessel cross-sectional area (CSA; square millimeter) for all 359 smokers in the range 0–20 mm^2. Results are provided for each lobe. The *color-coded line* represents the median profile and the *dotted lines* the 25th and 75th percentile. The figure inserts for each plot represent an enhanced view of the blood vessel volume distribution in the range of 0–70 mm^2.

accompanied by reciprocal engorgement and dilation of the more central vasculature to accommodate a shift of blood from the lungs to the extraparenchymal intrathoracic vessels. Recent work by Wells and coworkers (38) suggests that such an increase in vessel caliber has significant prognostic value for the prediction of acute exacerbations of COPD. Further work is required to determine the associations between intraparenchymal and extraparenchymal vessel morphology and if

TABLE 2. BLOOD VESSEL VOLUME MEASURES IN NEVER-SMOKING CONTROL SUBJECTS AND SMOKERS

	Distribution of Blood Vessel Volume Measures							
Variable	Never-Smoking Control Subjects (*n* = 82)	Smoking Control Subjects (*n* = 104)	GOLD1 (*n* = 27)	GOLD2 (*n* = 90)	GOLD3 (*n* = 87)	GOLD4 (*n* = 51)	*P* Value*	*P* Value†
Current smokers	0	56	9	24	20	5		
Whole right lung								
TBV_{right}, ml	100.1 (86.0–107.2)	98.2 (81.9–111.4)	96.5 (83.0–114.8)	94.9 (78.2–117.4)	92.8 (78.5–109.6)	94.4 (75.5.3–117.5)	0.48	0.90
$BV5_{right}$,ml	56.9 (50.8–64.0)	54.8 (47.0–63.3)	55.8 (46.9–63.6)	53.3 (44.6–61.6)	48.6 (41.7–56.7)	49.1 (41.1–57.1)	0.15	0.03
$T^{issue}V_{right}$, ml	2.67 (2.31–3.10)	2.68 (2.26–3.14)	2.86 (2.43–3.37)	2.54 (2.29–3.23)	2.46 (2.18–2.77)	2.46 (2.09–2.95)	0.98	0.002
Right upper lobe								
TBV_{RUL}, ml	33.2 (29.4–40.4)	31.4 (27.5–38.0)	33.4 (30.0–39.6)	36.5 (29.9–42.0)	35.0.6 (27.9–44.8)	35.9 (28.9–43.1)	0.15	0.43
$BV5_{RUL}$, ml	20.9 (17.9–24.3)	19.7 (16.6–23.2)	20.9 (17.1–22.6)	21.6 (17.9–24.9)	19.7 (16.0–24.0)	18.8 (16.0–23.5)	0.05	0.42
$T^{issue}V_{RUL}$, ml	0.94 (0.79–1.12)	0.97 (0.82–1.19)	1.16 (0.91–1.35)	1.09 (0.87–1.33)	1.02 (0.83–1.26)	1.01 (0.81–1.25)	0.23	0.09
Right lower lobe								
TBV_{RLL}, ml	49.7 (44.5–56.2)	50.1 (42.4–58.2)	52.7 (39.6–61.6)	46.6 (39.4–57.7)	45.6 (37.1–51.1)	43.7 (376–55.8)	0.80	0.38
$BV5_{RLL}$, ml	28.4 (25.0–31.6)	27.6 (23.1–32.3)	26.9 (22.3–32.4)	24.3 (20.4–29.6)	23.4 (19.3–27.4)	21.6 (18.3–27.7)	0.39	0.002
$T^{issue}V_{RLL}$, ml	1.26 (1.12–1.50)	1.27 (1.05–1.46)	1.32 (1.07–1.57)	1.16 (0.99–1.39)	1.06 (0.91–1.27)	1.08 (0.93–1.21)	0.51	0.0003

Definition of abbreviations: BV5 = pulmonary blood vessel volume in vessels less than 5 mm^2; GOLD = Global Initiative for Chronic Obstructive Lung Disease; RLL = right lower lobe; RUL = right upper lobe; TBV = total intraparenchymal blood vessel volume.

Volumes are presented for the whole right lung and for the right upper and right lower lobes.

Volumes are presented in milliliters as medians and interquartile ranges.

**P* value for difference in medians between never-smoking control subjects and smoking control subjects (smokers with normal lung function).

†*P* value for trend test across GOLD 1–4.

TABLE 3. BLOOD VESSEL VOLUME RATIOS FOR THE NEVER-SMOKERS AND SMOKERS

Variable	Distribution of Blood Vessel Volume Ratios							
	Never-Smoking Control Subjects	Smoking Control Subjects	GOLD1	GOLD2	GOLD3	GOLD4	*P* Value*	*P* Value†
Whole right lung								
$BV5_{right}/TBV_{right}$	0.58 (0.55–0.61)	0.57 (0.54–0.60)	0.56 (0.52–0.58)	0.55 (0.52–0.59)	0.53 (0.49–0.56)	0.52 (0.47–0.54)	0.25	<0.0001
$BV5_{right}/T^{issue}V_{right}$	0.021 (0.019–0.024)	0.020 (0.018–0.023)	0.019 (0.016–0.021)	0.019 (0.018–0.022)	0.019 (0.017–0.022)	0.019 (0.017–0.023)	0.25	0.34
Right upper lobe								
$BV5_{RUL}/TBV_{RUL}$	0.62 (0.59–0.66)	0.61 (0.58–0.65)	0.60 (0.56–0.63)	0.59 (0.55–0.63)	0.56 (0.53–0.60)	0.55 (0.51–0.60)	0.15	<0.0001
$BV5_{RUL}/T^{issue}V_{RUL}$	0.022 (0.020–0.026)	0.020 (0.017–0.024)	0.018 (0.016–0.022)	0.019 (0.017–0.022)	0.020 (0.016–0.022)	0.019 (0.017–0.022)	0.001	0.37
Right lower lobe								
$BV5_{RLL}/TBV_{RLL}$	0.56 (0.53–0.59)	0.56 (0.52–0.58)	0.53 (0.50–0.58)	0.53 (0.50–0.57)	0.51 (0.47–0.54)	0.49 (0.45–0.52)	0.46	<0.0001
$BV5_{RLL}/T^{issue}V_{RLL}$	0.022 (0.019–0.025)	0.022 (0.019–0.025)	0.020 (0.017–0.022)	0.021 (0.019–0.025)	0.020 (0.019–0.024)	0.021 (0.019–0.023)	0.68	0.51

Definition of abbreviations: $BV5_{right}/TBV_{right}$ = blood vessel volume less than 5 mm^2 in the whole right lung divided by the total intraparenchymal blood vessel volume in the whole right lung; $BV5_{RUL}/TBV_{RUL}$ = blood vessel volume less than 5 mm^2 in the right upper lobe divided by the total intraparenchymal blood vessel volume in the right upper lobe; $BV5_{RLL}/TBV_{RLL}$ = blood vessel volume less than 5 mm^2 in the right lower lobe divided by the total intraparenchymal blood vessel volume in the right lower lobe; $BV5_{right}/T^{issue}V_{right}$ = blood vessel volume less than 5 mm^2 in the whole right lung divided by the total nonvascular tissue volume in the whole right lung; $BV5_{RUL}/T^{issue}V_{RUL}$ = blood vessel volume less than 5 mm^2 in the right upper lobe divided by the nonvascular tissue volume of the right upper lobe; $BV5_{RLL}/T^{issue}V_{RLL}$ = blood vessel volume less than 5 mm^2 in the right lower lobe divided by the nonvascular tissue volume of the right lower lobe; GOLD = Global Initiative for Chronic Obstructive Lung Disease; RLL = right lower lobe; RUL = right upper lobe.

Volumes are presented as medians and interquartile ranges.

**P* value for difference in medians between never-smokers and smoking control subjects (smokers with normal lung function).

†*P* value for trend test across GOLD 1–4.

intraparenchymal vascular morphology is associated with acute exacerbations of COPD.

The TBV_{global} and $BV5_{global}$ were variably associated with D_{LCO}, resting oxygen saturation, and 6-MWD in univariate models. Generally, those subjects with greater TBV_{global} or $BV5_{global}$ tended to have less impairment according to those clinical measures but these observations were not consistent. It is possible that these associations could in part be attributed to total body size rather than disease state. For example, a taller individual with longer legs and larger lungs and thus more intraparenchymal pulmonary vasculature is likely to have a greater 6-MWD independent of disease state. Such anthropomorphic explanations could also be ascribed to the association of the $BV5_{global}$ and the D_{LCO} because the latter was an absolute value not expressed as a percent of predicted.

After an examination of the absolute measures of blood vessel volumes we created lobe-specific ratios of the distal blood volume to the total lobar blood volume. We did this to effectively remove the influence of lung volume on our measures. Using this measure we found that those with the lowest distal to TBV ratio tended to have a lower FEV_1 expressed as a percent of the predicted value (i.e., more severe COPD) and greater manifestations of their disease, such as a lower oxygen saturation, a lower 6-MWD, a higher SGRQ total score, and a higher BODE index. These observations (lower oxygen saturation, lower 6-MWD, higher SGRQ total score, higher BODE score) persisted after adjustment for pertinent confounding variables, such as age, sex, height, and %LAA-950. The latter covariate was systematically included in all of these models to explore the association of vascular morphology after accounting for differences in emphysema. The associations between %LAA-950 and clinical outcomes (SGRQ total score and resting oxygen saturation) were no longer significant after adjusting for vascular morphology measurements for all the lobes. Although there may be residual confounding effects, we contend that CT measures of vascular morphology are not simply a surrogate for standard densitometrically assessed emphysema but rather contain unique, clinically relevant information that may be further explored.

We also created lobe-specific ratios of the distal blood volume to the nonvascular tissue volume for each lobe. We did this to

TABLE 4. UNIVARIATE ASSOCIATIONS BETWEEN COMPUTED TOMOGRAPHY–DERIVED MEASURES OF BLOOD VESSEL MORPHOLOGY AND SELECT MEASURES OF CHRONIC OBSTRUCTIVE PULMONARY DISEASE SEVERITY

	TBV_{global}	$BV5_{global}$	$T^{issue}V_{global}$	$BV5_{RUL}/TBV_{RUL}$	$BV5_{RLL}/TBV_{RLL}$	$BV5_{RUL}/T^{issue}V_{RUL}$	$BV5_{RLL}/T^{issue}V_{RLL}$
FEV_1 % predicted ($n = 359$)	$r = -0.004$, $P = 0.9328$	$r = 0.20$, $P = 0.0001$	$r = 0.17$, $P = 0.0016$	$r = 0.36$, $P < 0.0001$	$r = 0.39$, $P < 0.0001$	$r = 0.05$, $P = 0.3358$	$r = 0.042$, $P = 0.4222$
%LAA-950 ($n = 359$)	$r = -0.19$, $P = 0.0003$	$r = -0.37$, $P < 0.0001$	$r = -0.17$, $P = 0.0015$	$r = -0.32$, $P < 0.0001$	$r = -0.30$, $P < 0.0001$	$r = -0.24$, $P < 0.0001$	$r = -0.20$, $P = 0.0002$
D_{LCO} post-bronchodilator ($n = 134$)	$r = 0.17$, $P = 0.0561$	$r = 0.29$, $P = 0.0008$	$r = 0.58$, $P < 0.0001$	$r = 0.09$, $P = 0.3$	$r = 0.16$, $P = 0.06$	$r = -0.26$, $P = 0.003$	$r = -0.27$, $P = 0.0015$
Oxygen saturation ($n = 359$)	$r = -0.11$, $P = 0.04$	$r = 0.07$, $P = 0.19$	$r = 0.24$, $P < 0.0001$	$r = 0.31$, $P < 0.0001$	$r = 0.37$, $P < 0.0001$	$r = -0.15$, $P = 0.004$	$r = -0.17$, $P = 0.001$
6-MWD ($n = 352$)	$r = 0.07$, $P = 0.17$	$r = 0.23$, $P < 0.0001$	$r = 0.37$, $P < 0.0001$	$r = 0.20$, $P = 0.0002$	$r = 0.28$, $P < 0.0001$	$r = -0.15$, $P = 0.004$	$r = -0.17$, $P = 0.0006$
SGRQ score total ($n = 359$)	$r = 0.06$, $P = 0.26$	$r = -0.06$, $P = 0.26$	$r = -0.13$, $P = 0.0124$	$r = -0.20$, $P = 0.0002$	$r = -0.26$, $P < 0.0001$	$r = 0.11$, $P = 0.039$	$r = 0.1$, $P = 0.068$
BODE ($n = 350$)	OR, 1.09 (0.91–1.31); $P = 0.36$	OR, 1.47 (1.22–1.79); $P < 0.0001$	OR, 1.51 (1.25–1.84); $P < 0.0001$	OR, 1.57 (1.30–1.9); $P < 0.0001$	OR, 1.76 (1.45–2.14); $P < 0.0001$	OR, 0.98 (0.82–1.18); $P = 0.85$	OR, 0.96 (0.79–1.15); $P = 0.63$

Definition of abbreviations: %LAA-950 = percentage of low-attenuation areas less than −950 Hounsfield units; 6-MWD = 6-minute-walk distance; BODE = body mass index, airflow obstruction, dyspnea, and exercise capacity index; $BV5_{global}$ = blood vessel volume less than 5 mm^2; $BV5_{RLL}/TBV_{RLL}$ = blood vessel volume less than 5 mm^2 in the right lower lobe divided by the total intraparenchymal blood vessel volume in the right lower lobe; $BV5_{RUL}/TBV_{RUL}$ = blood vessel volume less than 5 mm^2 in the right upper lobe divided by the total intraparenchymal blood vessel volume in the right upper lobe; $BV5_{RUL}/T^{issue}V_{RUL}$ = blood vessel volume less than 5 mm^2 in the right upper lobe divided by the nonvascular tissue volume of the right upper lobe; $BV5_{RLL}/T^{issue}V_{RLL}$ = blood vessel volume less than 5 mm^2 in the right lower lobe divided by the nonvascular tissue volume of the right lower lobe; D_{LCO} = diffusing capacity of carbon monoxide; OR = odds ratio; SGRQ = St. George's Respiratory Questionnaire; TBV_{global} = total intraparenchymal blood vessel volume.

Data presented for the FEV_1 percent predicted %LAA-950, D_{LCO}, oxygen saturation, 6-MWD, and SGRQ score total are the univariate (Pearson) correlation coefficients. The relationships between the vascular covariates and the BODE are presented as odds ratios and 95% confidence intervals.

TABLE 5. SUMMARY OF MULTIVARIATE MODELS FOR BV5/TBV AND BV5/T^{ISSUE}V

	Predictors														
	D_{LCO} Post-bronchodilator ($n = 134$)			Oxygen Saturation ($n = 358$)			6-MWD (*ft*) ($n = 351$)			SGRQ Score Total ($n = 358$)			BODE* ($n = 349$)		
Models	Beta	*P* Value	R^2	Beta	*P* Value	R^2	Beta	*P* Value	R^2	Beta	*P* Value	R^2	Beta	*P* Value	R^2
RUL															
$BV5_{RUL}/TBV_{RUL}$	15.20	0.07	0.47	13.44	0.0003	0.46	270.29	0.4877	0.43	−14.40	0.4769	0.33	6.1	0.003	0.35
$BV5_{RUL}/T^{issue}V_{RUL}$	−512.6	<0.0001	0.57	−206.5	<0.0001	0.48	−9646.2	0.0335	0.44	758.89	0.0011	0.35	−68.9	0.005	0.35
RLL															
$BV5_{RLL}/TBV_{RLL}$	24.02	0.0021	0.51	16.51	<0.0001	0.48	730.4	0.0593	0.44	−43.17	0.0334	0.33	10.1	<0.0001	0.42
$BV5_{RLL}/T^{issue}V_{RLL}$	−378.4	<0.0001	0.55	−185.1	<0.0001	0.48	−14167	0.0003	0.45	483.05	0.0222	0.34	−107.5	<0.0001	0.42
RML															
$BV5_{RML}/TBV_{RML}$	4.35	0.38	0.48	0.54	0.84	0.44	−336.73	0.2140	0.44	0.28	0.9847	0.33	4.1	<0.0001	0.25
$BV5_{RML}/T^{issue}V_{RML}$	−553.2	<0.0001	0.57	−202.9	<0.0001	0.47	−17743	0.0002	0.46	691.41	0.0071	0.34	−95.3	0.0007	0.26
LUL															
$BV5_{LUL}/TBV_{LUL}$	18.62	0.0136	0.50	10.33	0.0042	0.46	536.4	0.1494	0.44	−19.63	0.3128	0.33	7.1	0.0003	0.34
$BV5_{LUL}/T^{issue}V_{LUL}$	−565.2	<0.0001	0.56	−261.7	<0.0001	0.49	−11908	0.0191	0.44	538.57	0.0453	0.33	−96.7	0.0008	0.34
LLL															
$BV5_{LLL}/TBV_{LLL}$	21.26	0.0029	0.51	11.45	0.0006	0.46	600.5	0.0786	0.44	−39.41	0.0287	0.33	11.2	<0.0001	0.43
$BV5_{LLL}/T^{issue}V_{LLL}$	−388.7	<0.0001	0.54	−256.6	<0.0001	0.50	−10218	0.0177	0.44	186.24	0.4138	0.33	−106.4	<0.0001	0.39
Right lung															
$BV5_{Right}/TBV_{Right}$	25.42	0.0068	0.50	17.58	<0.0001	0.47	528.65	0.2547	0.44	−35.40	0.1373	0.33	8.7	0.0003	0.42
$BV5_{Right}/T^{issue}V_{Right}$	−577.50	<0.0001	0.58	−235.37	<0.0001	0.48	−15843	0.0009	0.45	742.65	0.0029	0.34	−103.9	0.0001	0.43
Left lung															
$BV5_{Left}/TBV_{Left}$	23.14	0.0042	0.51	14.56	0.0002	0.47	725.42	0.0723	0.44	−37.78	0.0728	0.33	10.4	<0.0001	0.44
$BV5_{Left}/T^{issue}V_{Left}$	−542.35	<0.0001	0.56	−293.27	<0.0001	0.50	−12507	0.0128	0.44	394.03	0.1387	0.33	−81.9	0.004	0.42

Definition of abbreviations: %LAA-950 = percentage of low-attenuation areas less than −950 Hounsfield units; 6-MWD = 6-minute-walk distance; BODE = body mass index, airflow obstruction, dyspnea, and exercise capacity index; $BV5_{RLL}/TBV_{RLL}$ = blood vessel volume less than 5 mm^2 in the right lower lobe divided by the total intraparenchymal blood vessel volume in the right lower lobe; $BV5_{RUL}/TBV_{RUL}$ = blood vessel volume less than 5 mm^2 in the right upper lobe divided by the total intraparenchymal blood vessel volume in the right upper lobe; $BV5_{RUL}/T^{issue}V_{RUL}$ = blood vessel volume less than 5 mm^2 in the right upper lobe divided by the nonvascular tissue volume of the right upper lobe; $BV5_{RLL}/T^{issue}V_{RLL}$ = blood vessel volume less than 5 mm^2 in the right lower lobe divided by the nonvascular tissue volume of the right lower lobe; D_{LCO} = diffusing capacity of carbon monoxide; OR = odds ratio; SGRQ = St. George's Respiratory Questionnaire.

Note that the multivariate models varied in the covariates used for adjustment. These model differences in the inclusion of additional independent covariates were based on biologic plausibility. For example, height was included in models to predict the D_{LCO} and 6-MWD because taller people generally have a larger unadjusted D_{LCO} and can walk farther in 6 minutes. In contrast, height was not included in models to predict resting oxygen saturation because there is no biologically apparent link between the two.

Multivariate models were adjusted as follows. D_{LCO}: %LAA-950, sex, height, and age. Oxygen saturation: FEV_1 percent predicted, %LAA-950, and sex. 6-MWD: FEV_1 percent predicted, %LAA-950, sex, height, weight, and age. SGRQ score total: FEV_1 percent predicted, %LAA-950, sex, and age. BODE: %LAA-950, sex, and age.

*The multivariate models for BODE were performed using ordinal logistic regression with the Beta value obtained as the maximal likelihood estimate.

explore the clinical associations of a metric that we believed may reflect the matching (or disruption) of blood to tissue. In general, those who had a higher ratio of distal blood vessel to tissue volume had more functional impairment from their COPD. Most interesting were the observed associations between these measures and the D_{LCO} in the absence of a similar association between D_{LCO} and distal blood volume to the total blood volume ratios. The D_{LCO} is a measure of the ability of the lung to exchange gases as inferred from the transfer of carbon monoxide into the blood. Our results suggest that an excess of blood volume or more likely a deficiency of tissue per blood volume leads to impaired gas transfer. Further exploration of this concept in a cohort of individuals without COPD who have CT data and corresponding measures of D_{LCO} may provide insight into the optimal matching of blood and tissue in a healthy lung.

The mechanisms by which vascular morphology are linked with the clinical manifestations of disease cannot be ascertained from this cross-sectional investigation. Such requires additional mechanistic study but a possible common link to these processes is the heart. Recently, Barr and coworkers (39) reported in a population-based study that even those with mild emphysema had appreciable decreases in left ventricular filling on cardiac magnetic resonance imaging. Given our observed associations between emphysema and blood volume ratios it is possible that those with a reduced distal to total blood volume ratio experience impaired ventricular filling both at rest and with exercise. Such could explain the decreased 6-MWD, the increased SGRQ, and potentially even the increased BODE index. This conjecture is supported by prior observations that pulmonary vascular disease is an independent predictor of increased morbidity and mortality in patients with COPD (1–4).

There are limitations to this investigation that must be acknowledged including the method of image analysis. No attempt was made to differentiate the morphology of the pulmonary artery or venous circulatory systems. Certainly, additional medical conditions, such as isolated dysfunction of the left or right heart, could selectively affect the arteries or veins and the methodology presented in this manuscript is not able to delineate these effects. Further work must be done to develop an automated robust method for the separation of arteries and veins. It must be noted, however, that in our prior work investigating the relationship of CT measures of pulmonary vascular morphology and pulmonary artery pressures by RHC (24), no attempt was made to delineate artery from vein. This suggests that although there may be selective processes that affect the intraparenchymal veins or arteries, there is a more significant systematic change in pulmonary vascular remodeling in smokers with distal pruning of the vessels.

Despite the modest hemodynamic impact of pulmonary vascular disease in smokers, its morbidity and association with heightened risk of death strongly argues for therapeutic intervention. The only generally accepted treatment for this condition in smokers is supplemental oxygen (40–42). Additional studies of selective and nonselective vasodilators have yielded mixed

results (43–45). Although these therapies are generally found to be efficacious in reducing pulmonary artery pressure, there has been little benefit and frequently a deleterious impact on oxygenation and ventilation-perfusion matching. Elevated vascular resistance because of vessel elongation in the setting of hyperinflation may best be treated by deflation (medical or surgical), vessel narrowing and lumen encroachment by selective vasodilation, and widespread absence of a vascular bed caused by emphysema may be refractory to therapy or even predispose patients to hemodynamic compromise in the setting of aggressive titration of therapy. Herein we presented a first step toward a more comprehensive assessment of pulmonary vascular morphology. Further work toward a detailed knowledge of the types of vascular remodeling present, their association with both parenchymal and airway disease, and their clinical impact is essential for the development of better treatments for COPD.

Author disclosures are available with the text of this article at www.atsjournals.org.

References

1. Chatila WM, Thomashow BM, Minai OA, Criner GJ, Make BJ. Comorbidities in chronic obstructive pulmonary disease. *Proc Am Thorac Soc* 2008; 5:549–555.
2. Falk JA, Kadiev S, Criner GJ, Scharf SM, Minai OA, Diaz P. Cardiac disease in chronic obstructive pulmonary disease. *Proc Am Thorac Soc* 2008;5:543–548.
3. Chaouat A, Naeije R, Weitzenblum E. Pulmonary hypertension in COPD. *Eur Respir J* 2008;32:1371–1385.
4. Minai OA, Chaouat A, Adnot S. Pulmonary hypertension in COPD: epidemiology, significance, and management: pulmonary vascular disease: the global perspective. *Chest* 2010;137(Suppl. 6):39S–51S.
5. Oswald-Mammosser M, Weitzenblum E, Quoix E, Moser G, Chaouat A, Charpentier C, Kessler R. Prognostic factors in COPD patients receiving long-term oxygen therapy. Importance of pulmonary artery pressure. *Chest* 1995;107:1193–1198.
6. Kessler R, Faller M, Fourgaut G, Mennecier B, Weitzenblum E. Predictive factors of hospitalization for acute exacerbation in a series of 64 patients with chronic obstructive pulmonary disease. *Am J Respir Crit Care Med* 1999;159:158–164.
7. Traver GA, Cline MG, Burrows B. Predictors of mortality in chronic obstructive pulmonary disease. A 15-year follow-up study. *Am Rev Respir Dis* 1979;119:895–902.
8. Weitzenblum E, Hirth C, Ducolone A, Mirhom R, Rasaholinjanahary J, Ehrhart M. Prognostic value of pulmonary artery pressure in chronic obstructive pulmonary disease. *Thorax* 1981;36:752–758.
9. Burgess MI, Mogulkoc N, Bright-Thomas RJ, Bishop P, Egan JJ, Ray SG. Comparison of echocardiographic markers of right ventricular function in determining prognosis in chronic pulmonary disease. *J Am Soc Echocardiogr* 2002;15:633–639.
10. Incalzi RA, Fuso L, De Rosa M, Di Napoli A, Basso S, Pagliari G, Pistelli R. Electrocardiographic signs of chronic cor pulmonale: a negative prognostic finding in chronic obstructive pulmonary disease. *Circulation* 1999;99:1600–1605.
11. Cordasco EM, Beerel FR, Vance JW, Wende RW, Toffolo RR. Newer aspects of the pulmonary vasculature in chronic lung disease. A comparative study. *Angiology* 1968;19:399–407.
12. Scarrow GD. The pulmonary angiogram in chronic bronchitis and emphysema. *Proc R Soc Med* 1965;58:684–687.
13. Jacobson G, Turner AF, Balchum OJ, Jung R. Vascular changes in pulmonary emphysema. The radiologic evaluation by selective and peripheral pulmonary wedge angiography. *Am J Roentgenol Radium Ther Nucl Med* 1967;100:374–396.
14. Hale KA, Niewoehner DE, Cosio MG. Morphologic changes in the muscular pulmonary arteries: relationship to cigarette smoking, airway disease, and emphysema. *Am Rev Respir Dis* 1980;122:273–278.
15. Wright JL, Lawson L, Paré PD, Hooper RO, Peretz DI, Nelems JM, Schulzer M, Hogg JC. The structure and function of the pulmonary vasculature in mild chronic obstructive pulmonary disease. The effect of oxygen and exercise. *Am Rev Respir Dis* 1983;128:702–707.
16. Magee F, Wright JL, Wiggs BR, Paré PD, Hogg JC. Pulmonary vascular structure and function in chronic obstructive pulmonary disease. *Thorax* 1988;43:183–189.
17. Barberà JA, Riverola A, Roca J, Ramirez J, Wagner PD, Ros D, Wiggs BR, Rodriguez-Roisin R. Pulmonary vascular abnormalities and ventilation-perfusion relationships in mild chronic obstructive pulmonary disease. *Am J Respir Crit Care Med* 1994;149:423–429.
18. Santos S, Peinado VI, Ramírez J, Melgosa T, Roca J, Rodriguez-Roisin R, Barberà JA. Characterization of pulmonary vascular remodelling in smokers and patients with mild COPD. *Eur Respir J* 2002;19:632–638.
19. Washko GR. Rate of decline in FEV1: is emphysema the culprit? *Am J Respir Crit Care Med* 2012;185:2–3.
20. Mohamed Hoesein FA, de Hoop B, Zanen P, Gietema H, Kruitwagen CL, van Ginneken B, Isgum I, Mol C, van Klaveren RJ, Dijkstra AE, *et al.* CT-quantified emphysema in male heavy smokers: association with lung function decline. *Thorax* 2011;66:782–787.
21. Vestbo J, Edwards LD, Scanlon PD, Yates JC, Agusti A, Bakke P, Calverley PM, Celli B, Coxson HO, Crim C, *et al.*; ECLIPSE Investigators. Changes in forced expiratory volume in 1 second over time in COPD. *N Engl J Med* 2011;365:1184–1192.
22. Han MK, Kazerooni EA, Lynch DA, Liu LX, Murray S, Curtis JL, Criner GJ, Kim V, Bowler RP, Hanania NA, *et al.*; COPDGene Investigators. Chronic obstructive pulmonary disease exacerbations in the COPDGene study: associated radiologic phenotypes. *Radiology* 2011;261:274–282.
23. Matsuoka S, Washko GR, Dransfield MT, Yamashiro T, San Jose Estepar R, Diaz A, Silverman EK, Patz S, Hatabu H. Quantitative CT measurement of cross-sectional area of small pulmonary vessel in COPD: correlations with emphysema and airflow limitation. *Acad Radiol* 2010;17:93–99.
24. Matsuoka S, Washko GR, Yamashiro T, San Jose Estepar R, Diaz A, Silverman EK, Hoffman E, Fessler HE, Criner GJ, Marchetti N, *et al.*; National Emphysema Treatment Trial Research Group. Pulmonary hypertension and computed tomography measurement of small pulmonary vessels in severe emphysema. *Am J Respir Crit Care Med* 2010;181:218–225.
25. Regan EA, Hokanson JE, Murphy JR, Make B, Lynch DA, Beaty TH, Curran-Everett D, Silverman EK, Crapo JD. Genetic epidemiology of COPD (COPDGene) study design. *COPD* 2010;7:32–43.
26. Zach JA, Newell JD Jr, Schroeder J, Murphy JR, Curran-Everett D, Hoffman EA, Westgate PM, Han MK, Silverman EK, Crapo JD, *et al.*; COPDGene Investigators. Quantitative computed tomography of the lungs and airways in healthy nonsmoking adults. *Invest Radiol* 2012;47:596–602.
27. Standardization of spirometry, 1994 update. American Thoracic Society. *Am J Respir Crit Care Med* 1994;152:1107–1136.
28. American Thoracic Society. Lung function testing: selection of reference values and interpretative strategies. *Am Rev Respir Dis* 1991;144:1202–1218.
29. Jones PW, Quirk FH, Baveystock CM. The St George's respiratory questionnaire. *Respir Med* 1991;85(Suppl. B):25–31; discussion 33–27.
30. Mahler DA, Wells CK. Evaluation of clinical methods for rating dyspnea. *Chest* 1988;93:580–586.
31. Celli BR, Cote CG, Marin JM, Casanova C, Montes de Oca M, Mendez RA, Pinto Plata V, Cabral HJ. The body-mass index, airflow obstruction, dyspnea, and exercise capacity index in chronic obstructive pulmonary disease. *N Engl J Med* 2004;350:1005–1012.
32. Ross JC, San Jose Estepar R, Kindlmann G, Diaz A, Westin CF, Silverman EK, Washko GR. Automatic lung lobe segmentation using particles, thin plate splines, and maximum a posteriori estimation. *Med Image Comput Comput Assist Interv* 2010;13:163–171.
33. Washko GRHG, Hunninghake GM, Fernandez IE, Nishino M, Okajima Y, Yamashiro T, Ross JC, Estépar RS, Lynch DA, Brehm JM, *et al.*; COPDGene Investigators. Lung volumes and emphysema in smokers with interstitial lung abnormalities. *N Engl J Med* 2011;364:897–906.
34. Kindlmann GL, San José Estépar R, Smith SM, Westin CF. Sampling and visualizing creases with scale-space particles. *IEEE Trans Vis Comput Graph* 2009;15:1415–1424.
35. San Jose Estepar RRJ, Krissian K, Schultz T, Washko GR, Kindlmann GL. Computational vascular morphometry for the assessment of pulmonary vascular disease based on scale-space particles. In: Biomedical Imaging (ISBI), 2012 9th IEEE International Symposium on. IEEE; 2012. pp. 1479–1482.
36. Matsuoka S, Yamashiro T, Diaz A, Estépar RS, Ross JC, Silverman EK, Kobayashi Y, Dransfield MT, Bartholmai BJ, Hatabu H, *et al.* The relationship between small pulmonary vascular alteration and aortic

atherosclerosis in chronic obstructive pulmonary disease: quantitative CT analysis. *Acad Radiol* 2011;18:40–46.

37. Wan ES, Hokanson JE, Murphy JR, Regan EA, Make BJ, Lynch DA, Crapo JD, Silverman EK; COPDGene Investigators. Clinical and radiographic predictors of GOLD-unclassified smokers in the COPDGene study. *Am J Respir Crit Care Med* 2011;184:57–63.
38. Wells JM, Washko GR, Han MK, Abbas N, Nath H, Mamary AJ, Regan E, Bailey WC, Martinez FJ, Westfall E, *et al.*; COPDGene Investigators; ECLIPSE Study Investigators. Pulmonary arterial enlargement and acute exacerbations of COPD. *N Engl J Med* 2012;367:913–921.
39. Barr RG, Bluemke DA, Ahmed FS, Carr JJ, Enright PL, Hoffman EA, Jiang R, Kawut SM, Kronmal RA, Lima JA, *et al.* Percent emphysema, airflow obstruction, and impaired left ventricular filling. *N Engl J Med* 2010;362:217–227.
40. Weitzenblum E, Sautegeau A, Ehrhart M, Mammosser M, Pelletier A. Long-term oxygen therapy can reverse the progression of pulmonary hypertension in patients with chronic obstructive pulmonary disease. *Am Rev Respir Dis* 1985;131:493–498.
41. Medical Research Council Working Party. Long term domiciliary oxygen therapy in chronic hypoxic cor pulmonale complicating chronic bronchitis and emphysema: report of the Medical Research Council Working Party. *Lancet* 1981;1:681–686.
42. Nocturnal Oxygen Therapy Trial Group. Continuous or nocturnal oxygen therapy in hypoxemic chronic obstructive lung disease: a clinical trial. *Ann Intern Med* 1980;93:391–398.
43. Archer SL, Mike D, Crow J, Long W, Weir EK. A placebo-controlled trial of prostacyclin in acute respiratory failure in COPD. *Chest* 1996; 109:750–755.
44. Vonbank K, Ziesche R, Higenbottam TW, Stiebellehner L, Petkov V, Schenk P, Germann P, Block LH. Controlled prospective randomised trial on the effects on pulmonary haemodynamics of the ambulatory long term use of nitric oxide and oxygen in patients with severe COPD. *Thorax* 2003;58:289–293.
45. Roger N, Barberà JA, Roca J, Rovira I, Gómez FP, Rodriguez-Roisin R. Nitric oxide inhalation during exercise in chronic obstructive pulmonary disease. *Am J Respir Crit Care Med* 1997;156:800–806.